Supporting information

Covalent Organic Frameworks with Interlayer Fixed Pt Atoms for Efficient Electrocatalytic Hydrogen Evolution

Daqing Fan, Weiwen Wang, Tian Ma, Xianglin Luo, Chao He, Xikui Liu*, and Shuang Li**

D. Fan, W. Wang, Dr. T. Ma, Prof. X. Luo, Dr. C. He, Prof. X. Liu, and Prof. S. Li
College of Polymer Science and Engineering, State Key Laboratory of Polymer Materials Engineering, Sichuan University, Chengdu 610065, China
E-mail: shuang.li@scu.edu.cn

Supplementary Experiment Sections

1. Materials

All chemicals and reagents were analytical grade or better and used without further purification, and ultrapure water was used throughout all experiments. 2,4,6-tris(4-aminophenyl)-1,3,5-triazine(TAPTA), 1,3,5-benzenetricarbaldehyde were purchased from Alfa Aesar and used as received. Tetrahydrofuran, 1,4-Dioxane, 1,3,5-Trimethylbenzene, and glacial acetic acid were purchased from Aladdin. Chloroplatinic acid hydrate was purchased from Energy Chemical.

2. Synthetic procedure

Synthesis of TTB-COF, TTB-COP. The centrifuge tube was preloaded with 2,4,6-tris(4-aminophenyl)-1,3,5-triazine (70.9 mg) and 1,3,5-benzenetricarboxaldehyde (32.45 mg), respectively. Acetonitrile (10 ml) was then added, and the solution containing the building blocks was mixed well. Subsequently, 2 ml of glacial acetic acid was added and shaken vigorously for 6 hours at room temperature. The resulting yellow precipitate, collected by centrifugation, was washed

with anhydrous ethanol and 1,4-dioxane, respectively. The obtained precipitate was dispersed in a round-bottomed flask containing 1,4-dioxane (8 mL), trimethyl benzene (2 mL) (4:1 v/v), water, and glacial acetic acid. The resulting suspension was sealed and aged at 80 °C for 120h. By keeping the ratio of precursors constant, samples named TTB-COP were synthesized and employed for 72h. The yellow powder was collected by centrifugation washed several times with a large amount of tetrahydrofuran and dried under vacuum at 100 °C for 6 h.

Synthesis of Pt@TTB-COF, Pt@TTB-COP. 20 mg of H_2PtCl_4 and 30 mg of TTB-COF(TTB-COP) were mixed in 30 ml of anhydrous ethanol. The mixture was heated to 60 °C with stirring and constant temperature for 6h.

3. Characterization

The morphology of the as-prepared catalysts was observed by scanning electron microscopy (SEM, Apreo S HiVoc, Thermo Fisher Scientific) and transmission electron microscope (TEM, FEI Talos F200X). The phase composition was identified by a Dandong Haoyuan DX-2700BH X-ray diffractometer using Cu Kα radiation (λ = 0.15406 nm). X-ray photoelectron Spectra (XPS) were measured on a K-Alpha X-ray photoelectron spectrometer system (Thermo Scientific) with a Hemispheric 180° dual-focus analyzer with a 128-channel detector. The X-ray monochromator was microfocused Al Kα radiation. For the measurement, the prepared powder samples were pressed and loaded on carbon taps and then pasted onto the sample holder for measurement. The data were collected with an X-ray spot size of 400 μm, 20 scans for the survey, and 50 scans for the regions. Scanning transmission electron microscopy (STEM) images and electron energy loss spectroscopy (EELS) elemental mapping were acquired on a Cs-corrected (S)TEM (FEI Titan Cubed Themis G2 300). The X-ray absorption spectroscopy (XAS) measurements were recorded at the X-ray absorption spectroscopy beamline of the Australian Synchrotron (ANSTO) in fluorescence mode. The radiation was monochromatized by a Si (111) double-crystal monochromator. XANES and EXAFS data reduction and analysis were processed by Athena software.

4. Electrochemical Measurements.

In a typical preparation of catalyst ink, the catalyst powder (10 mg) was blended with 100 μL Nafion solution (5 wt%) and 900 μL ethanol in an ultrasonic bath. 5 μL of catalyst ink was then pipetted onto the glassy carbon (GC) surface, leading to a catalyst loading of ~ 0.254 mg/cm^2. Commercially available 20 wt % Pt/C on carbon black was measured with the same loading amount for comparison.

All the electrochemical measurements were carried out in a conventional three-electrode cell using the Gamry reference 600 workstations (Gamry, USA) at room temperature. A commercial RHE electrode was used as the reference electrode, and the graphite rod was used as the counter electrode. The Ag/AgCl reference electrode calibrated with RHE in 0.5 M H_2SO_4 was used as a reference electrode for long-term stability measurement. A glassy carbon (GC) RDE electrode with an area of 0.196 cm^2 served as the substrate for the working electrode to evaluate the HER activities of various catalysts. The electrochemical experiments were conducted in an Ar-saturated 0.5 M H_2SO_4 electrolyte. The HER polarization curves of different catalysts with real-time IR-corrected by Gamry reference 600 potentiostats at a resistance of 4.4 ohms. The RDE measurements were conducted at a rotating speed of 1600 rpm with a sweep rate of 10 mV/s.

Electrochemical impedance spectroscopy (EIS) was carried out with a potentiostatic EIS method with a DC voltage of −0.015 V vs. RHE in an Ar-saturated 0.5 M H_2SO_4 electrolyte from 100 kHz to 0.1 Hz with a 10 mV AC potential at 1600 rpm. The stability tests for the catalysts were conducted using chronopotentiometry at the constant working current densities of 10 mA/cm^2. Electrochemically active surface area (ECSA) was estimated by measuring the capacitance of the double layer at the solid-liquid interface with cyclic voltammetry. The measurement was performed in a potential window of 0.35–0.55 V vs. RHE, where the Faradic current on the working electrode was negligible. The series of scan rates ranging from 50 to 300 mV s^{-1} was applied to build a plot of the charging current density differences against the scan rate. The slope of the obtained linear curve was twice the double-layer capacitance (Cdl), which was used to estimate ECSA.

Supplementary Figures.

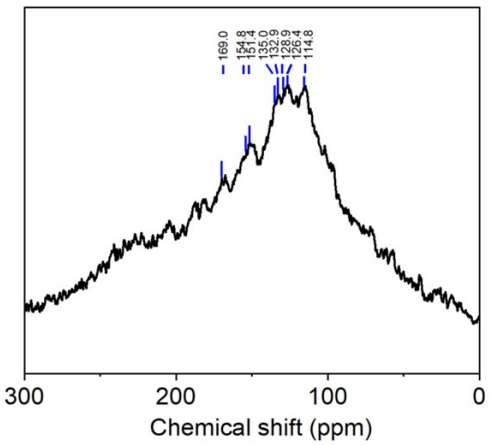

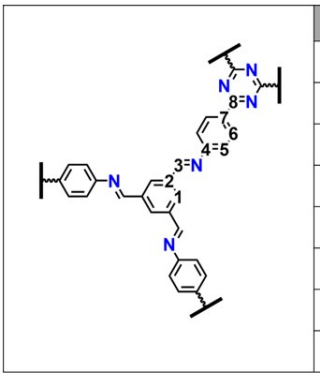

Assignment	Signal(ppm)
1	135.0
2	132.9
3	154.8
4	151.4
5	114.8
6	126.4
7	128.9
8	169.0

Figure S1. ^{13}C CP-MAS solid-state NMR spectra of TTB-COF and molecular model of TTB-COF and ^{13}C NMR spectrum peak assignment.

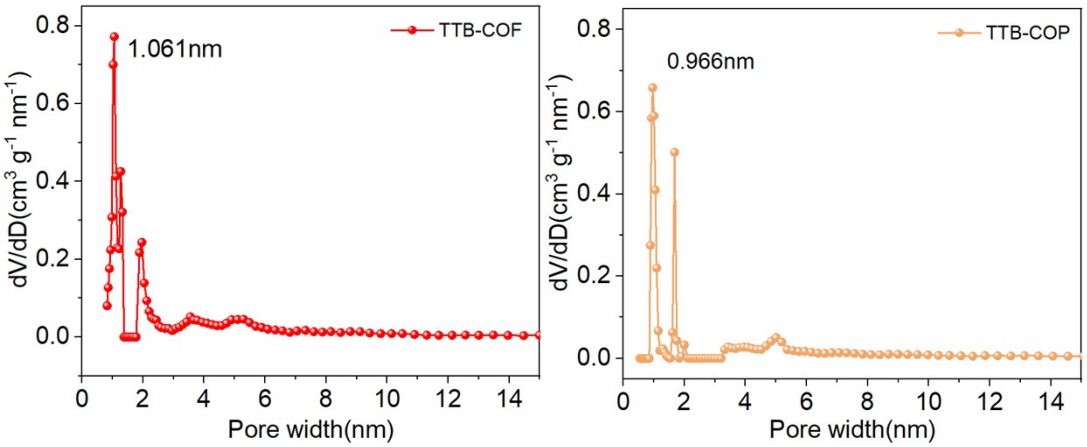

Figure S2. The distribution of pore sizes for TTB-COF and TTB-COP at 77K

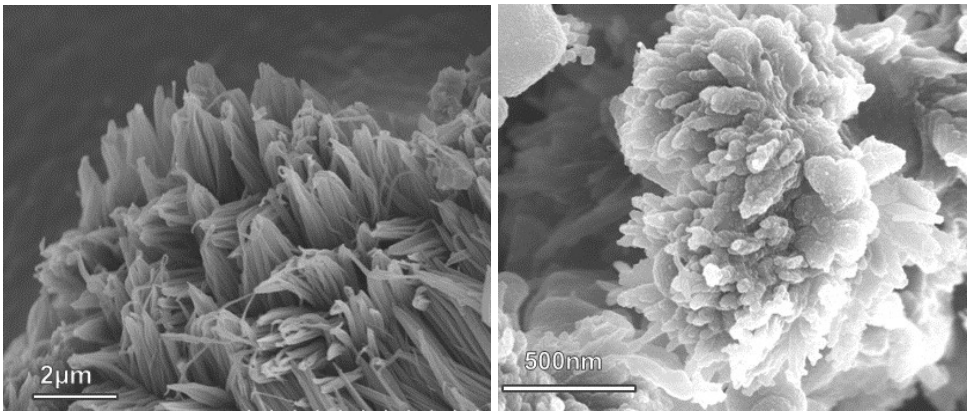

Figure S3. SEM images of Pt@TTB-COF, and Pt@TTB-COP.

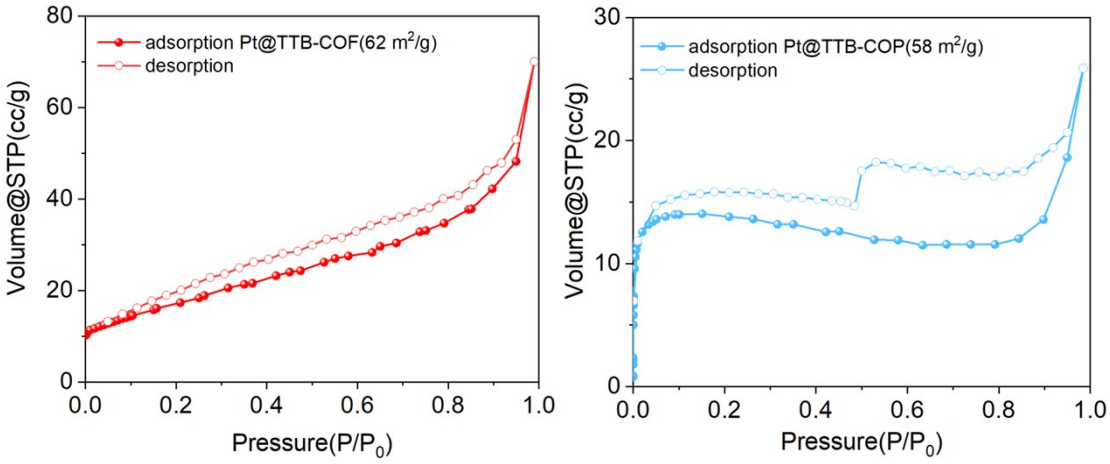

Figure S4. N_2 sorption isotherms for Pt@TTB-COF and Pt@TTB-COP at 77K.

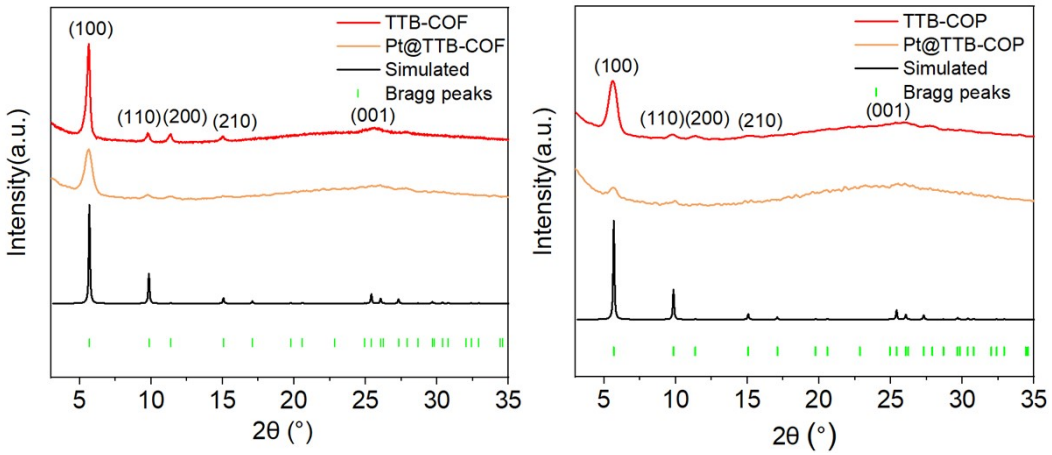

Figure S5. PXRD patterns and Pawley refinement of TTB-COF, Pt@TTB-COF, TTB-COP, and Pt@TTB-COP.

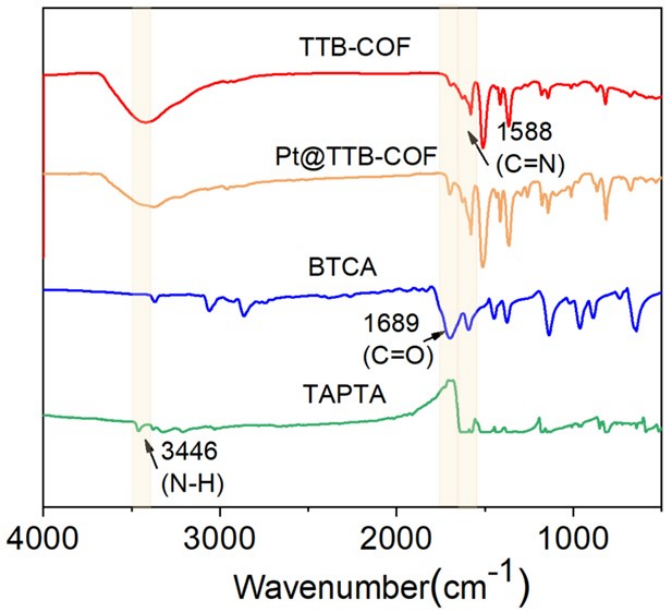

Figure S6. The FTIR spectra of TTB-COF and its corresponding monomers.

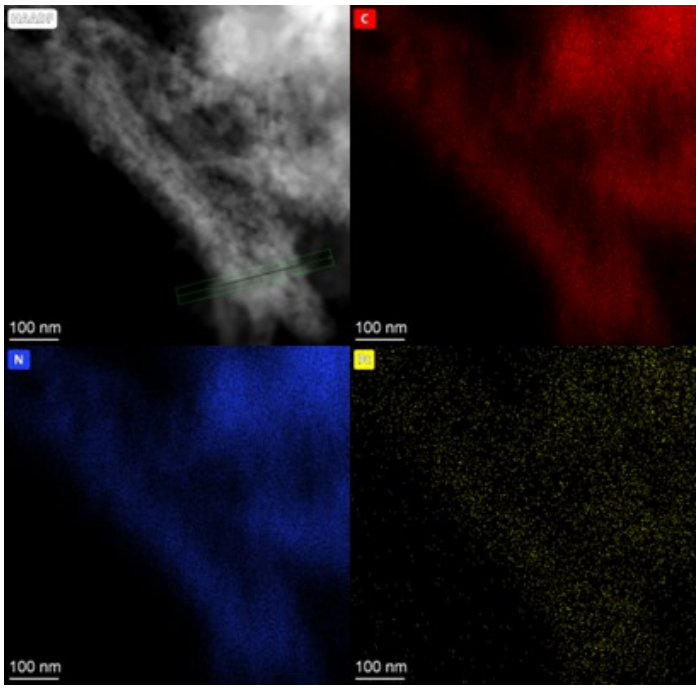

Figure S7. The element mapping of C, N, and Pt for Pt@TTB-COF

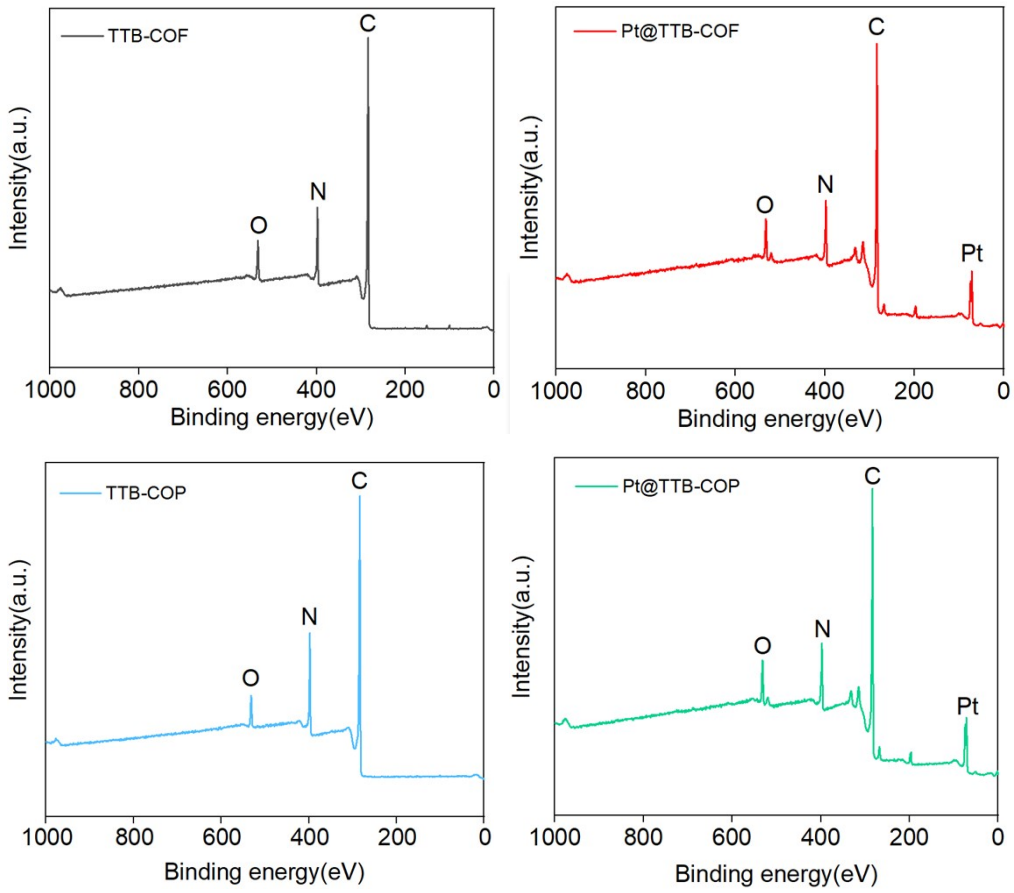

Figure S8. XPS wide-scan survey of TTB-COF, Pt@TTB-COF, TTB-COP and Pt@TTB-COP.

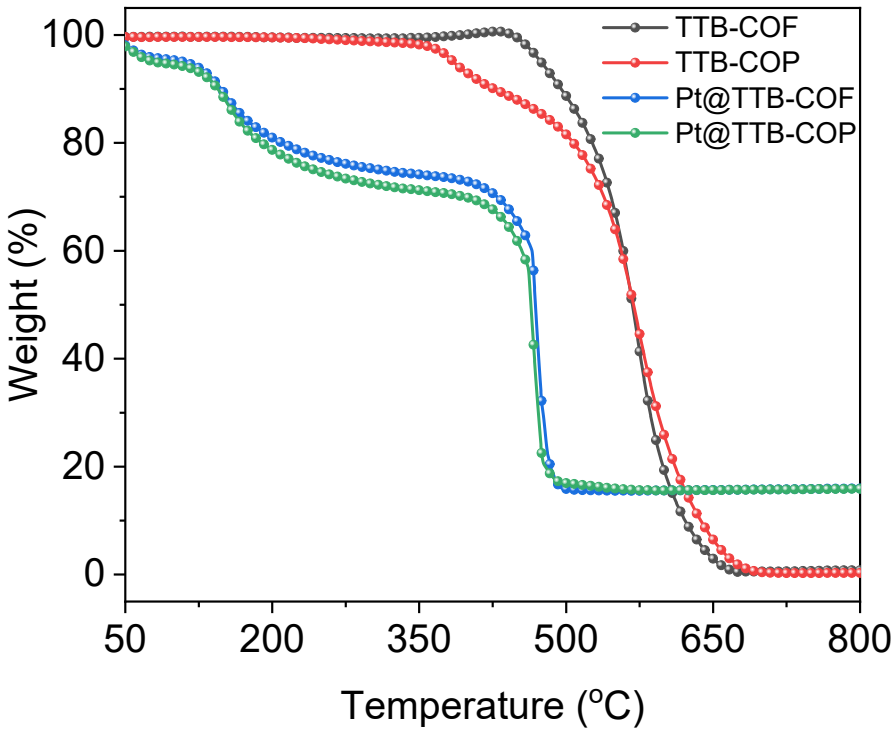

Figure S9. TGA analysis of the TTB-COF, TTB-COP, Pt@TTB-COF, and Pt@TTB-COP measured in air.

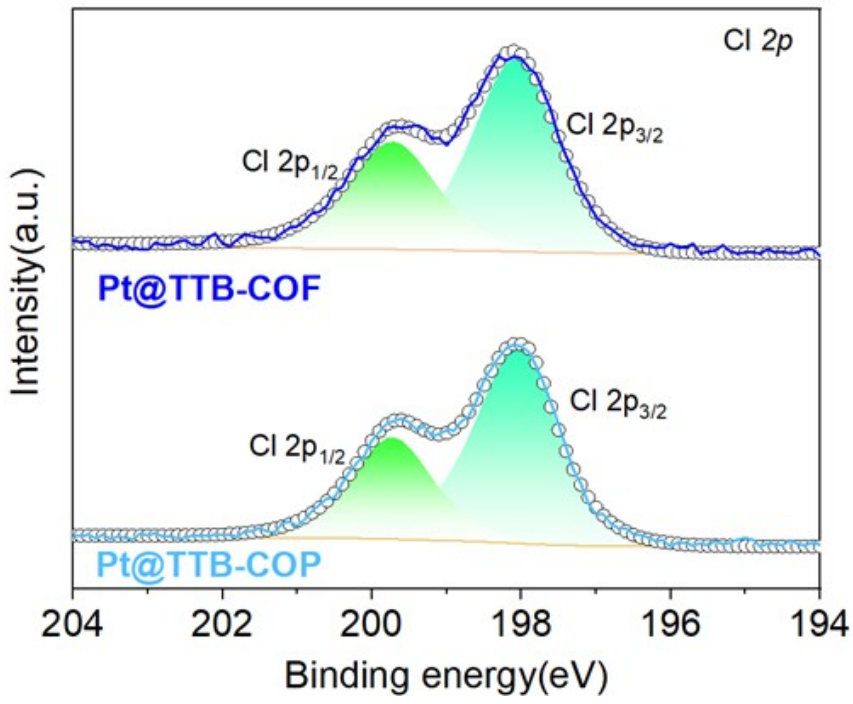

Figure S10. Cl *2p* XPS spectra of Pt@TTB-COF and Pt@TTB-COP.

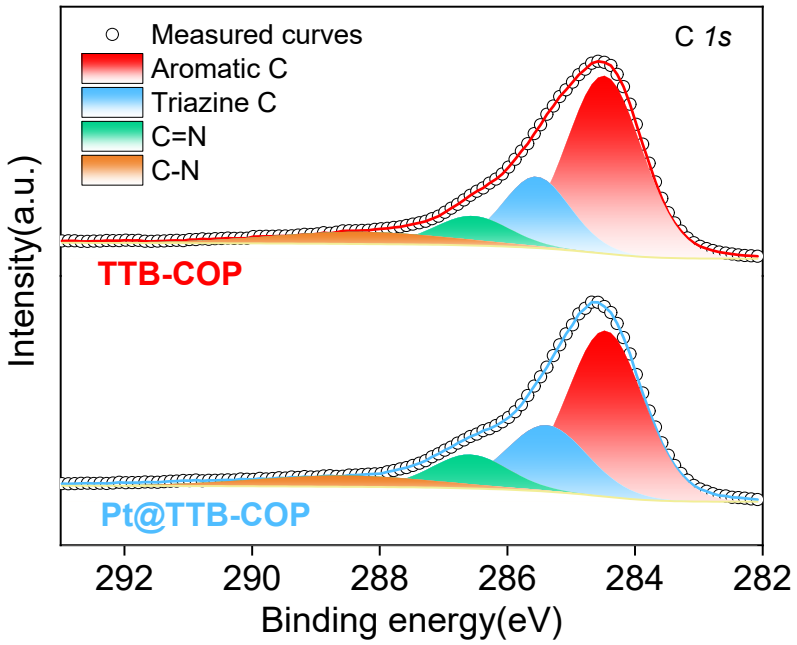

Figure S11. C 1s XPS spectra of TTB-COP and Pt@TTB-COP.

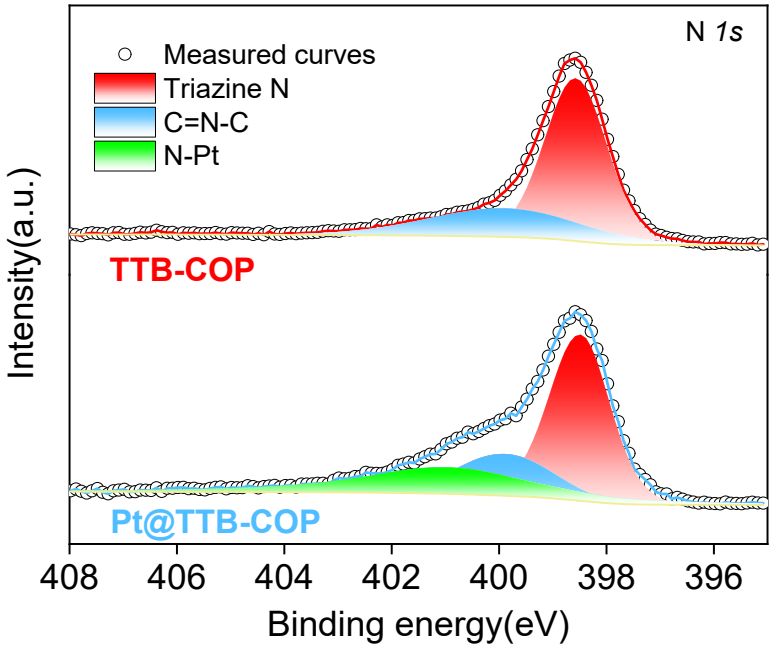

Figure S12. N 1s XPS spectra of TTB-COP and Pt@TTB-COP.

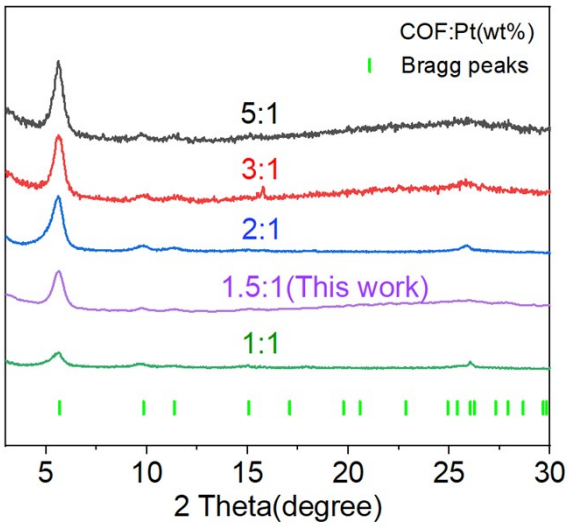

Figure S13. PXRD images of different Pt complexation ratios.

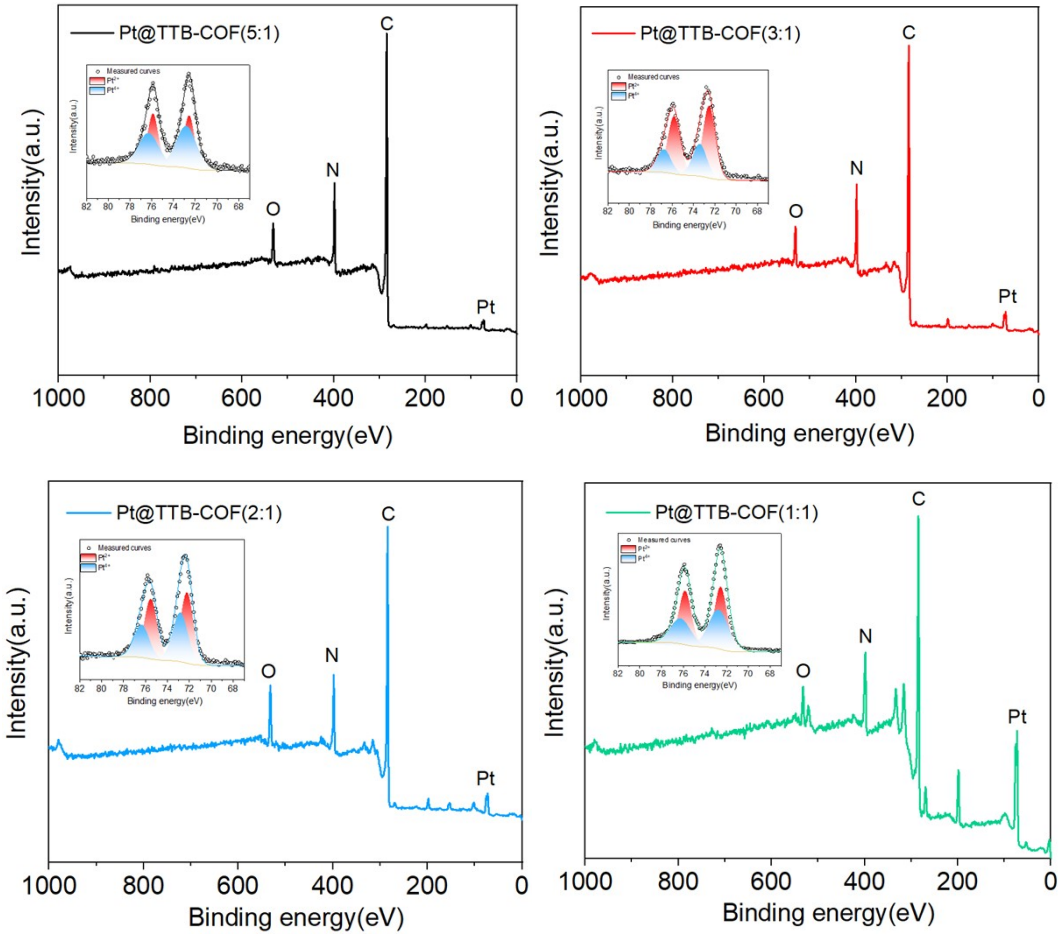

Figure S14. XPS wide-scan survey of Pt@TTB-COF(COF:Pt=5:1); Pt@TTB-COF(COF:Pt=3:1); Pt@TTB-COF(COF:Pt=2:1); Pt@TTB-COF(COF:Pt=1:1).

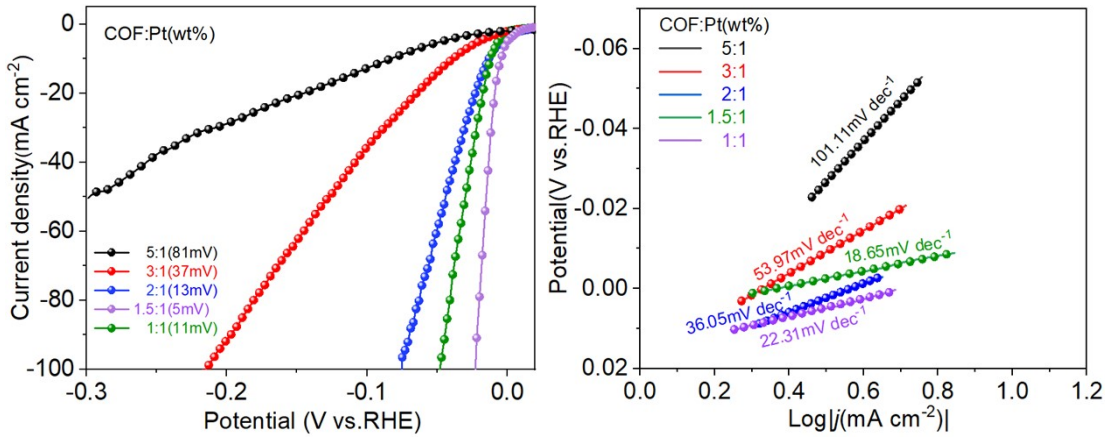

Figure S15. LSV polarization curves and corresponding Tafel slopes for Pt@TTB-COF different Pt content ratios.

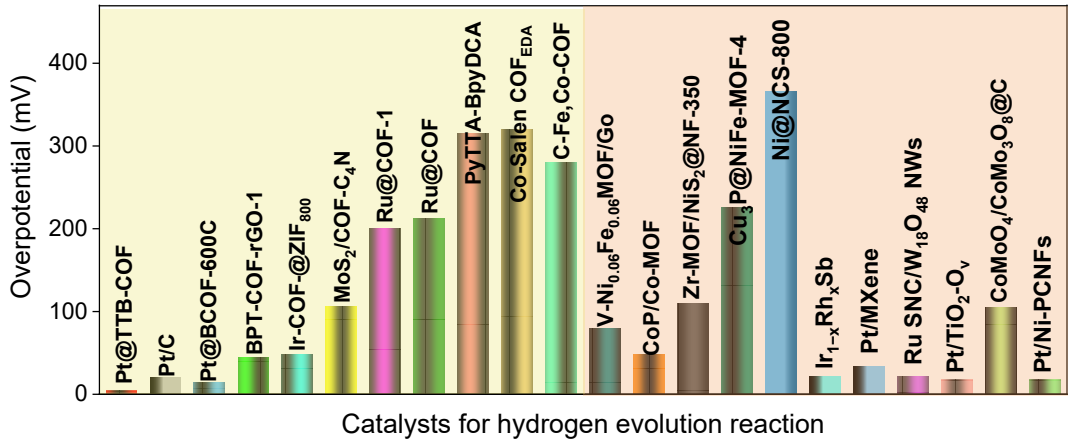

Figure S16. Comparison of the HER activity of Pt@TTB-COF and other previously reported materials.

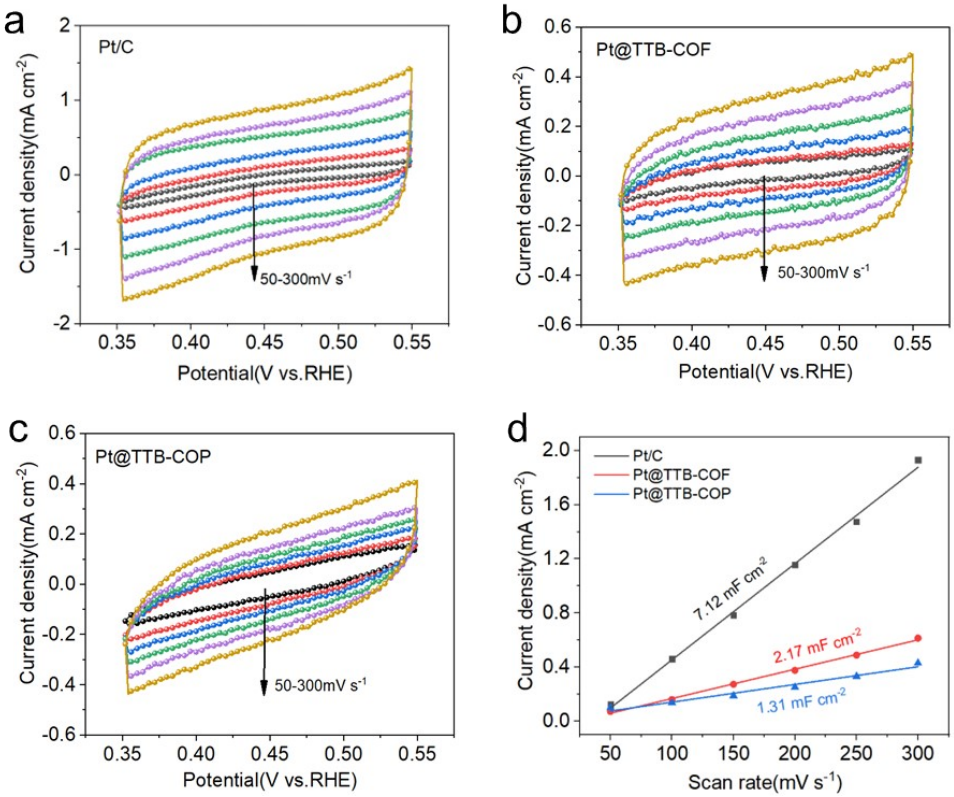

Figure S17. CV curves of a) Pt/C, b) Pt@TTB-COF, and c) Pt@TTB-COP under different scan rates. d) C_{dl} plots extrapolated from the CV curves.

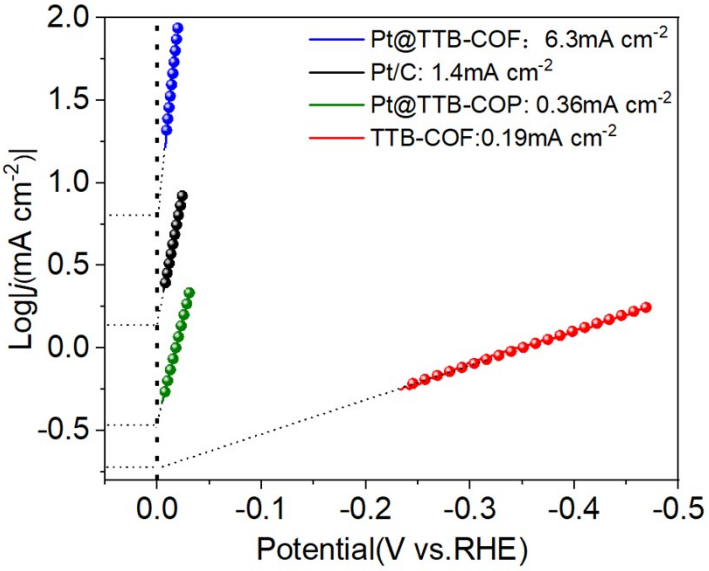

Figure S18. Exchange current density images and values for Pt@TTB-COF, Pt/C, etc.

Table S1. XPS measurements of TTB-COF, Pt@TTB-COF, TTB-COP and Pt@TTB-COP (wt%).

	C	N	O	Pt	Cl
TTB-COF	76.82	15.41	7.77		
Pt@TTB-COF	59.89	11.69	6.68	15.78	5.96
TTB-COF	76.12	17.48	6.40		
Pt@TTB-COP	55.32	12.00	6.60	15.36	10.73

Table S2. XPS measurements of TTB-COF, Pt@TTB-COF, TTB-COP, and Pt@TTB-COP (at%).

	C	N	O	Pt	Cl
TTB-COF	80.14	13.78	6.08		
Pt@TTB-COF	76.86	12.87	6.43	1.25	2.59
TTB-COF	79.36	15.63	5.01		
Pt@TTB-COP	73.62	13.69	6.59	1.26	4.84

Table S3. EXAFS fitting parameters at the Pt L_3-edge for various samples (S_0^2=0.61).

Sample	Shell	N^a	R(Å)^b	σ^2(Å^2)^c	ΔE_0(eV)^d	R factor
Pt@TTB-COF	Pt-N	1.0	1.97	0.0021	8.763	0.0178
	Pt-Cl	3.0	2.29	0.0047		
Pt foil	Pt-Pt	12.0	2.76	0.0043	8.423	0.0029
$PtCl_4$	Pt-Cl	4.0	2.28	0.0041	2.415	0.0036

[a]N: coordination numbers; [b]R: bond distance; [c] σ^2: Debye-Waller factors; [d]ΔE_0: the inner potential correction. R factor: goodness of fit. S_0^2 was set to 0.61, according to the experimental EXAFS fit of Pt foil by fixing CN as the known crystallographic value.

Table S4. Summary of recently reported COF or MOF-based HER catalysts in acidic electrolyte.

No	Year	Material	Feature	Performance	Ref
1	This work	COF	Pt@TTB-COF	0.5M H_2SO_4, η_{10}: 5mV	This work
2	2022	COF	Pt@BCOF-600C	0.5M H_2SO_4, η_{10}: 14.5mV	*J. Am. Chem. Soc.* **2022**, 144, 43, 19973–19980
3	2022	COF	BPT-COF-rGO-1	0.5M H_2SO_4, η_{10}: 45mV	*Angew. Chem. Int. Ed.* **2022**, 61, e202113067
4	2022	COF	Ir-COF@ZIF_{800}	0.5M H_2SO_4, η_{10}: 48mV	*Chem. Commun.*, **2022**, 58, 13214–13217
5	2023	COF	N-MoS_2/COF-C_4N	0.5M H_2SO_4, η_{10}: 106mV	*Catalysts* **2023**, 13, 90
6	2022	COF	Ru@COF-1	0.5M H_2SO_4, η_{10}: 200mV	*Small* **2022**, 18, 2107750
7	2022	COF	PyTTA-BPyDCA	0.5M H_2SO_4, η_{10}: 315mV	*Nat Commun* 13, 1411 (**2022**)
8	2022	COF	Co-Salen COF_{EDA}	0.5M H_2SO_4, η_{10}: 320mV	*Adv. Sci.* **2022**, 9, 2105912
9	2020	COF	Ru@COF	1.5M H_2SO_4, η_{10}: 212mV	*ChemNanoMat* **2020**, 6, 99–106
10	2023	MOF	Zr-MOF/NiS_2 @NF-350	0.5M H_2SO_4, η_{10}: 110mV	*Journal of Colloid and Interface Science* 640 (**2023**) 820–828
11	2022	MOF	Cu_3P@NiFe-MOF-4	0.5M H_2SO_4, η_{10}: 226mV	*Catalysis Letters* (**2022**) 152:3825–3832
12	2023	MOF	Ni@NCS-800	0.5M H_2SO_4, η_{10}: 366mV	*Applied Surface Science* 616 (**2023**) 156499
13	2022	Other	$Ir_{1-x}Rh_xSb$	0.5M H_2SO_4, η_{10}: 22mV	*Adv. Energy Mater.* **2022**, 12, 2200855
14	2022	Other	Pt/MXene	0.5M H_2SO_4, η_{10}: 34mV	*Adv. Funct. Mater.* **2022**, 32, 2110910
15	2023	Other	Pt/TiO_2-O_V	0.5M H_2SO_4, η_{10}: 18mV	*Angew. Chem. Int. Ed.* **2023**, 62, e202300406